FERMION MONTE CARLO

MALVIN H. KALOS[‡] AND FRANCESCO PEDERIVA
Laboratory of Atomic and Solid State Physics,
Center for Theory and Simulation in Science and Engineering,
Cornell University, Ithaca, NY 14853

Abstract.

We review the fundamental challenge of fermion Monte Carlo for continuous systems, the "sign problem", and some of the proposals that have been made for its solution, including some approximate schemes and others whose computing requirements grow exponentially. The issue is to find the lowest eigenmode of the Schrödinger equation in many dimensions that has a special inversion of sign- antisymmetry in the exchange of pairs of coordinates. Thus the function sought is not everywhere positive. We also describe a class of methods that depend upon the use of correlated dynamics for ensembles of walkers that carry opposite signs. We discuss the algorithmic symmetry between such walkers that must be broken to create a method that is both exact and as effective as for treating the fundamental symmetric solution. We explain the concept of marginally correct dynamics. Stable overlaps with an antisymmetric trial function given by such dynamics correspond to the lowest antisymmetric mode. As an elementary example, we show how walkers correlated in a purely geometric way can find an antisymmetric wave function for a particle in a parallelogram. Many-body harmonic oscillator problems are particularly tractable: Their stochastic dynamics permits the use of regular geometric structures for the ensembles, structures that are stable when appropriate correlations are introduced, and thereby avoid the decay of signal-to-noise that is a normal characteristic of the sign problem. Finally, we outline a new generalization of the method for arbitrary potentials and describe its success in treating few-electron systems, free fermions, and ^{3}He.

[‡]Present address: Lawrence Livermore National Laboratory, Livermore CA 94550

1. Introduction

It has been clear through four decades of development of Quantum Monte Carlo, and its application to many and diverse systems that fermions are much more difficult than bosons to treat in an effective general way[1, 2, 3].

An effective solution is one that has the following properties in common with boson Monte Carlo programs: (a) convergence to the exact fermion ground state without uncontrolled approximations, and (b) errors that decrease asymptotically with computational time t as $t^{-\frac{1}{2}}$. "Uncontrolled approximations" include for example the use of variational methods and constrained path or "fixed-node" calculations. The errors involved in these procedures cannot be assessed directly from the calculations nor be reduced to an arbitrary degree by more computing. We seek an "intrinsically exact" method whose outcome does not require validation by experiment.

The importance of developing an exact many-fermion Monte Carlo method is hard to overstate: At present all numerical methods for multi-fermion systems have uncontrolled approximations of some sort. It is highly desirable at the very least that accurate benchmarks be developed. A sufficiently fast method might be incorporated into dynamics calculations.

Current algorithms satisfy (a) or (b) but not both. All use random walks in configuration space that establish a many-dimensional distribution proportional to the many-body wave function. Averages over walker positions using approximate many-body wave functions yield Monte Carlo estimates of overlap integrals with the fermion wave function, from which results of physical interest, such as energy eigenvalues can be inferred. Projecting with properly antisymmetrized wave functions will converge to the fermion ground state, but without some restriction on the walks, the mean values of the integrals decay exponentially relative to their statistical errors. This is a kind of statistical instability, and criterion (b) above is not satisfied. Conversely, fixed-node calculations are stable but are approximations unless the nodes are exact: Criterion (a) is violated.

For our purposes, the differences between Green's Function Monte Carlo (GFMC)[4] and Diffusion Monte Carlo (DMC)[1, 5, 6] are irrelevant. What is essential is that both exploit the analogy of the imaginary-time Schrödinger equation to a diffusion equation in which the physical potential plays the role of generalized absorption. They use random walks in configuration space whose asymptotic many-dimensional distributions are proportional to the many-body wave function. Monte Carlo programs that follow these forms of stochastic dynamics will generate such many-body distributions numerically, from which quantities of physical interest may be inferred, by projection using an antisymmetrized trial function.

These random walks are local. That is, the rules and functions that govern the behavior of each walker depend purely on its position. The boundary condition prescribed by the Pauli principle, namely that the wave function be antisymmetric under the exchange of like-spin fermions, is a global condition that cannot readily be enforced within the framework of independently diffusing objects. Fixed-node calculations use an approximate version of a global condition but no way has yet been found to adapt the nodes to the exact form required.

We have been exploring algorithms in which the dynamics of walkers that carry opposite signs are correlated in such a way that the marginal behavior of any one walker is the same as if its partners were absent. The diffusion processes are negatively correlated so that opposite walkers eventually meet and cancel. The results converge to the exact fermion ground state, and their errors decrease asymptotically as $t^{-\frac{1}{2}}$.

This paper constitutes a review of the general issues and of the development of correlated walks. In the next sections we will recall some of the approaches that have been used for computing properties of many-fermion systems. We will then introduce a new general algorithm that has been successfully applied to physical systems and that appears to satisfy both conditions a) and b) listed above. That is to say that it appears to be general and exact.

2. Approximate methods for Fermion Monte Carlo

Several approximate methods have been developed for computing properties of many-fermion systems. A class of these relies on an approximation (which in principle can be very precise) of the many-body wave function of the system (with its nodal surfaces) and includes variational calculations, fixed-node DMC and GFMC, and the mirror potential method. Transient estimation attempts to extract information on the ground state beyond the variational level by propagating the diffusion for a limited imaginary time after removing the fixed-node constraint.

2.1. VARIATIONAL METHODS

The variational method[3] consists in building a class of trial wave functions Ψ_T for a many-body system, which depend on a set of variational parameters $\{\alpha\}$, and computing the quantum average of the Hamiltonian operator applied to this trial state

$$E_T\{\alpha\} = \frac{\langle \Psi_T | \hat{H} \Psi_T \rangle}{\langle \Psi_T | \Psi_T \rangle}. \tag{1}$$

Since this always gives an upper bound, the best ground-state energy within this class of trial functions is the minimum with respect to the parameters.

For some purposes (e.g., for importance sampling the random walk used in GFMC or DMC) a more suitable trial function is that which minimizes the variance of the "local energy", $\hat{H}\Psi_T/\Psi_T$. A typical variational wave function for a many-fermion system is of the form:

$$\Psi_T(\vec{R}, \{\alpha\}) = \psi(\vec{r}_1 \dots \vec{r}_N) \det ||\chi_j(\vec{r_i})|| \tag{2}$$

where the function $\psi(\vec{r}_1 \dots \vec{r}_N)$ describes the quantum correlations due to the interaction. The determinant of some suitable single particle wave functions $\chi_j(\vec{r_i})$ enforces the correct antisymmetry properties in the wave function. This method has been successfully applied to many physical problems, but we will not review here the applications and results, which can be found in the literature. In particular significant results have been obtained in the study of many-electron atoms [7], liquid[8] and solid[9] ^{3}He, and nuclei [10].

2.2. FIXED-NODE METHODS

The variational method provides a basis for what can be considered the most widely used approximation in fermion calculations. Because the exact antisymmetric solution Ψ_0 changes sign on application of an odd permutation among indistinguishable particles and because it is continuous, it must vanish on a $3N-1$ dimensional manifold in the $3N$ dimensional space of the coordinates in an N-body system[12]. These manifolds (the "nodal structure") are usually unknown. We can always imagine that the antisymmetric ground state Ψ_0 can be represented as the difference of two positive functions ϕ^+ and ϕ^- each delimited by the nodal structure.

$$\Psi_0 = \phi^+ - \phi^- \tag{3}$$

Each of the two positive functions can therefore be imagined as derived by a distribution of walkers ("positive" walkers for ϕ^+ and "negative" walkers for ϕ^-), and can be thought as densities for their populations. The knowledge of the nodal structure coming from the solution of an accurate variational calculation Ψ_T can be exploited to optimize separately the positive and the negative parts of the wave function using a projection algorithm. In this case one solves the problem by Diffusion Monte Carlo or Green's Function Monte Carlo as in the bosonic case, with the boundary condition that the solution vanish at the nodal surface of Ψ_T. If the nodal structure coincides with the exact one, the solution is exact. It can be proved that the energy lies above the ground state (and in this respect the method is still variational), but it is lower than the variational result E_T, and the difference from the exact result is second order in $(\Psi_T - \Psi_0)$[13]. This method has been very widely applied to the same systems quoted in the variational case. The application of very sophisticated optimization techniques in the variational method has produced results that in many cases are very close to experiment. Still this remains a variational method: The approximation to the nodal structure is uncontrolled, and the quality of the calculation can be justified only a posteriori, by comparing with experiment. Different versions of the "fixed-node" idea are also used in Path Integral Monte Carlo (PIMC) calculations, under the name of constrained path methods.

2.3. TRANSIENT ANALYSIS

In the fixed-node approximation the populations of positive and negative walkers never overlap. What happens if we relax the boundary conditions at the nodal surface? In this case the populations are free to propagate. All the excited components decay with respect to the ground state during the propagation, and the densities will eventually converge to:

$$\phi^{\pm}(\vec{R}) \rightarrow c_{S0}\Psi_{S0}(\vec{R}) \pm c_0 e^{-(E_0-E_{S0})\tau}\Psi_0. \tag{4}$$

where τ is imaginary time, and where the subscript $S0$ refers to the symmetric ground state. Since the difference $E_0 - E_{S0}$ always positive, the component along the antisymmetric ground state disappears, and the two populations of positive and negative walkers take on the distribution of the symmetric ground state and overlap completely with each other. This can be expected if one notes that exchanging ϕ^+ and ϕ^- does not affect at all the Schrödinger equation and its solution, or in other words, that there is a *plus-minus symmetry* intrinsic in the problem, which is somehow spontaneously broken by fermions.

It is still possible to obtain information on the antisymmetric ground state. In fact, if we multiply both members of Eq. (4) by an antisymmetric trial function Ψ_T, and integrate over $\vec{R}$, the symmetric components disappear:

$$\int \Psi_T(\vec{R})\phi^+(\vec{R})d\vec{R} \rightarrow c_0 e^{-(E_0-E_{S0})\tau}\langle\Psi_T|\Psi_0\rangle \tag{5}$$

The same happens if we consider $\hat{H}\Psi_T$. So the average value of the Hamiltonian becomes:

$$\frac{\int \hat{H}\Psi_T(\vec{R})\phi^+(\vec{R})d\vec{R}}{\int \Psi_T(\vec{R})\phi^+(\vec{R})d\vec{R}} \rightarrow \frac{\langle\hat{H}\Psi_T|\Psi_0\rangle}{\langle\Psi_T|\Psi_0\rangle} = E_0 \tag{6}$$

Evaluating the previous quotient from configuration coming from a free propagation of the walkers gives the correct average energy. What about the variance of this estimator? Let us consider the variance of the denominator. It is proportional to:

$$\int \Psi_T^2(\vec{R})\phi^+(\vec{R})d\vec{R} - \left[\int \Psi_T(\vec{R})\phi^+(\vec{R})d\vec{R}\right]^2 \tag{7}$$

The square of Ψ_T in the first integral is a *symmetric* function. This means that while the signal from Eq. (5) decays, the *noise remains constant*, and consequently the *signal to noise ratio grows exponentially*. However, each evaluation of the integral in Eq. (6) is an upper bound for the exact eigenvalue E_0, and these upper bounds converge to E_0[11]. If the signal to noise ratio is still acceptable after some imaginary time steps, it is possible to give an estimate of the asymptotic limit of the upper bounds. This is a form of transient estimates. While in principle it could give the exact answer, it cannot be predicted in advance that the convergence can be seen clearly before the errors grow too large. Nevertheless some useful results, for instance in nuclei [10] and for the electron gas[14], have been achieved.

2.4. MIRROR POTENTIALS

From the discussion in the previous point it becomes clear that a major condition for stability (meaning a constant signal to noise ratio throughout the calculation) is to be able to generate populations of positive and negative walkers that have a constant non-zero overlap with an antisymmetric function. Let us consider the coupled equation for two functions Ψ^+ and Ψ^-:

$$\begin{aligned} \hat{H}(\vec{R}) + C(\vec{R})\Psi^-(\vec{R})\Psi^+(\vec{R}) &= E\Psi^+(\vec{R}) \\ \hat{H}(\vec{R}) + C(\vec{R})\Psi^+(\vec{R})\Psi^-(\vec{R}) &= E\Psi^-(\vec{R}) \end{aligned} \tag{8}$$

These equations have the property that the difference of the solutions $\Psi^+(\vec{R}) - \Psi^-(\vec{R})$ satisfies the Schrödinger equation for the original Hamiltonian. The populations distributed as Ψ^+ and Ψ^- are distinct and stable. The term $C(\vec{R})\Psi^{\mp}$ can be interpreted as a repulsive "mirror" potential for the walkers of opposite sign. The strength of $C(\vec{R})$ determines how well separated the two populations are. A possible procedure for finding a solution for the coupled equations (8) consists in introducing an approximate solution for Ψ^-, solving for Ψ^+ and iterating the procedure. This method has been tested in two simple cases, the one-dimensional infinite square well and the three dimensional harmonic oscillator[15].

Mirror potentials introduce an explicit attempt for breaking the plus-minus symmetry. However, note that the exchange of the two populations has no effect on the paired equations (8). So while an overlap with an antisymmetric function is guaranteed at any time, the sign of the overlap can change; nothing prevents the two populations from exchanging into each other. Stability is not guaranteed, and the method as it stands can again be used only in conjunction with the use of variational functions. However, the ideas underlying the mirror potential will suggest part of the approach to a general exact method to be discussed later.

3. Correlated Ensembles

From the discussion in the previous section we understand that in order to construct an algorithm that generates a population of walkers with a stable overlap with an antisymmetric function it is necessary to break the symmetry between the distributions of walkers carrying opposite sign. This demands that the two distributions not be independent. It is therefore useful to introduce correlations between walkers of opposite sign, possibly using different correlations depending on the position and orientation of the pair [5, 16, 18]. If the interchange of the two members in a pair changes the dynamics for the evolution of the pair then the symmetry is broken in a simple way. This gives one possibility for building a stable fermion algorithm. As shown by Kalos and Schmidt[17], if a stable overlap with an antisymmetric function is generated, and if the marginal dynamics for any single walker is correct, then the overlap is correct. "Correct marginal dynamics" means that the behavior of a walker in a correlated ensemble cannot be distinguished from that of a single free walker, except possibly for cancellation of opposite walkers. In more formal terms the distribution of the walker obtained after integrating the many-walker distribution over all the other coordinates must be equal to the distribution of a single independent walker. In diffusion Monte Carlo it is in general enough to move each walker according to the usual drift-diffusion-branching procedure to ensure correct marginal dynamics. Since the Monte Carlo estimates of overlap integrals are linear in the probability density, they are not changed by correlations among walkers. For that reason, marginally correct dynamics is sufficient to ensure correct expected values of the integrals.

The drift is determined by the importance function used. To ensure long-lived pairs it is necessary that the branching be reduced, and not be strongly dependent on the particular member of the pair. For these reasons the importance function should be close to the *symmetric* ground state of the problem. In model problems the exact solution, if available, can be used. Nevertheless we will see later that it is not necessary or indeed desirable to respect this condition, and differential branching (which can produce unpaired walkers) can be easily handled.

A class of correlations compatible with this scheme can be obtained introducing relations among the diffusion vectors $\vec{U}$ for the members of an ensemble. Suppose that we have a pair of walkers $(\vec{R}^+, \vec{R}^-)$, and that $(\vec{U}^+, \vec{U}^-)$ are the respective diffusion vectors at a given step. $\vec{U}^+$ and $\vec{U}^-$ come from the same Gaussian distribution. If we sample one of the two vectors, say $\vec{U}^+$, the choices $\vec{U}^- = \vec{U}^+$ or $\vec{U}^- = -\vec{U}^+$ both guarantee correct dynamics for $\vec{R}^-$. We refer to the first choice as "parallel" dynamics and to the second as "antiparallel" dynamics.

A more interesting kind of correlation between the Gaussian vectors is "reflected dynamics". In this case we consider the line joining the two members of a pair and the hyperplane orthogonal to this line. Then make $\vec{U}^-$ the reflection of $\vec{U}^+$ in that plane. The crucial fact about this dynamics is that the relative distance of the two members $|\vec{R}^+ - \vec{R}^-|$ for a finite size system is a bounded random walk in one dimension, so that the two walkers are guaranteed to meet (and to cancel) at a finite time. This cancellation property does not depend strongly on the dimensionality of the system, and can be made more efficient if the pairs $(\vec{R}^+, \vec{R}^-)$ are sampled from the kernel constructed from the difference of the Green's functions centered in the new positions $\vec{R'}^+$ and $\vec{R'}^-$ respectively. Although this property seems very promising, it is not enough to guarantee stability for the algorithm. Again, pair by pair, the exchange of the two members does not change the dynamics, and the plus-minus symmetry is not broken. One possible choice is, as mentioned above, to apply different correlated dynamics in different ways for interchanged pairs or pairs of special orientation. We refer to this as "symmetry breaking by geometry".

3.1. PARTICLE IN A PARALLELOGRAM

A paper by Liu, Zhang and Kalos [18] was the first illustration of the idea of symmetry breaking by geometry, in this case for the first excited state of a particle whose wave function vanishes on the boundary of a parallelogram as shown in Fig. 1a. Take the origin of the coordinates at the middle of lm. Construct pq to be orthogonal to lm at the origin. Neither of these lines can be a nodal surface. The parallelogram is then divided into four regions, A,B,C,and D. Region A is subdivided into two subregions A1 and A2 as shown. D is the reflection of A1 in lm and also the reflection of B in pq. Walkers are started only in A region, and then diffuse and multiply along the way. Some of them will reach the exterior of the region where they disappear because of the boundary conditions. Suppose that a walker arrives at the diagonal lm (Fig. 1b). A pair is created, each member with weight 1/2, and the two future paths are constructed to be the reflection of each other in line lm. In Fig. 1b one of the two members of a pair touches the boundary lq of the region D. That walker is killed. Let us consider now the case of a walker crossing the pq line coming from the A region. Again a partner following reflected dynamics in pq is created (Fig. 1c) In both cases we have two possibilities, shown in Fig. 1d. If one of the walkers in a pair touches the exterior boundaries of the parallelogram, the other member of the pair survives in region A and keeps contributing. If one of the members touches the pq or the lm lines, the same happens to the partner. The resulting ensemble of walkers consists of points that

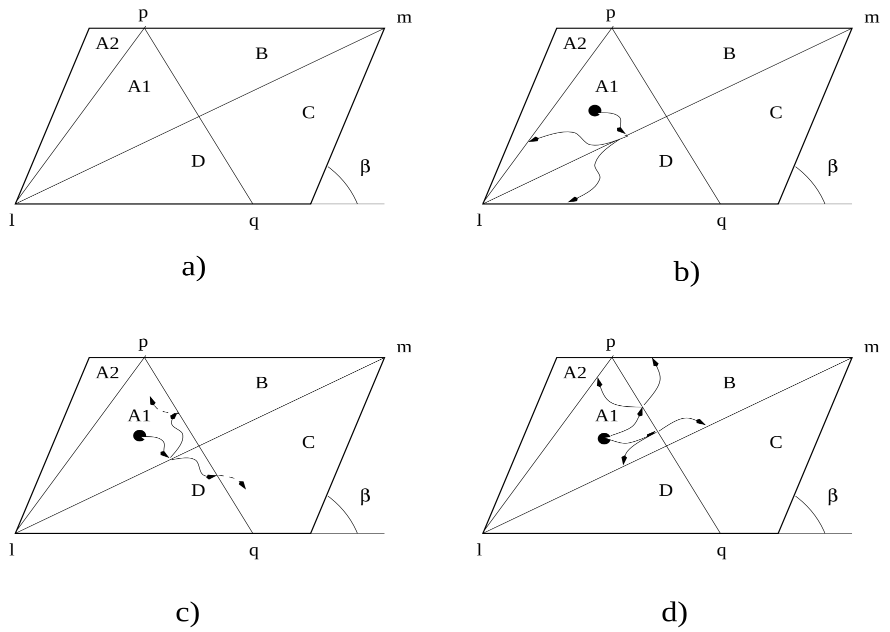

Figure 1. Geometrical construction for the parallelogram divided in four regions A,B,C,D, and possible evolutions of a walker touching their boundaries.

are reciprocally inversion points with respect to the origin, and will give zero total contribution for any test function that has inversion symmetry. Furthermore, future steps of any inverted pair can be correlated to keep them inverted, so that all future contributions vanish. Therefore, when a walker (pair) touches for the second time one of the internal boundaries, the pair is removed. The outcome is that no walkers ever enter region C and the population distribution has nonzero overlap with any function whose average value is different from zero in the region considered. Branching provides the creation of new walkers and pairs.

This scheme was implemented to study the first excited state of the Schrödinger equation for a particle in a parallelogram, using a Domain Green's Function Monte Carlo scheme, and the details of the simulation can be found in ref. [18]. The first excited state has inversion symmetry, with respect to the origin, namely $\Psi(\vec{R}) = -\Psi(-\vec{R})$. In a test on a rectangular box (for which the solution is known) the discrepancy between the computed eigenvalue and the analytic result is within the errorbars. For the parallelogram a trial function of the following form was used:

$$\Psi_T(x,y) = x(b^2 - y^2)[y\cos\beta - (x+a)\sin\beta][y\cos\beta - (x-a)\sin\beta] \quad (9)$$

where a and b are the side lengths and β is the angle characterizing the parallelogram. This function vanishes at the boundaries, and has a nodal line in $x = 0$, which is wrong for this problem. The simulation performed with the above scheme moves the nodal line away from $x = 0$. The algorithm in this case works very well. Its importance lies in its implication that purely geometric correlations –that have no immediate connection with the symmetries of the Hamiltonian– can create a stable antisymmetric distribution.

3.2. HARMONIC OSCILLATOR

3.2.1. *One dimensional case*

The concepts of symmetry breaking by geometry and by use of correlated walkers can perhaps be better understood using the elementary example of the one-dimensional harmonic oscillator[19]. We want to find the first antisymmetric solution using Diffusion Monte Carlo. Let us consider a pair of walkers $\{x_0^+, x_0^-\}$, both evolving through a drift-diffusion-branching process that is determined by an importance or "guiding" function equal to the ground state $e^{-x^2/2}$. If $\Delta\tau$ is the time step, then drift will transform x into $e^{-\Delta\tau}x = \rho$. We now use parallel dynamics for the pair of walkers, meaning that each walker moves by the same amount u, distributed as a Gaussian of mean zero and variance $(1-\rho^2)/2$. The evolution after k steps will be:

$$c_0^+ \to \rho x_0^+ \rho + u_1 \to \rho[\rho x_0^+ \rho + u_1] + u2 \to \ldots \rho^k x_0^+ + \sum_{l=1}^{k} \rho^{k-l} u_l \quad (10)$$

and asymptotically:

$$\lim_{k\to\infty} \sum_{n=0}^{k-1} \rho^n u_{(k-n)} \quad (11)$$

The same applies to x_0^-. The distance Δx between the two walkers decreases by a factor of $e^{-\Delta\tau}$, and tends to 0. per step. Branching can be replaced by the use of a weight factor different from unity because the trial energy is that of the excited state while the local energy is that of the ground state. In the case of the first excited state, for instance, the walkers have to be reweighted by the factor $e^{\Delta\tau}$ at each step. After a time τ, the total weight of a pair will be therefor $W_0 e^{\tau}$ where W_0 is the initial weight.

At each step the product $\Delta x_k W_k$ is a constant equal to $\Delta x_0 W_0$. Moreover, the asymptotic distribution of the walkers will be the same for the two members of the pair and equal to $\psi_0^2(x) = e^{-x^2}$. If we compute the overlap of the distribution generated by the pairs with any antisymmetric function f_A we will have

$$\begin{aligned}\int f_A(x)\psi_A(x) &= \int \frac{f_A(x)}{\psi_0(x)}\psi_0(x)\psi_a(x)dx \\ &= \sum_k W_k\left[\frac{f_A(x_k^+)}{\psi_0(x_k^+)} - \frac{f_A(x_k^-)}{\psi_0(x_k^-)}\right] \\ &\to \sum_k W_k \Delta x_k \frac{d}{dx}\left[\frac{f_A(x)}{\psi_0(x)}\right]\end{aligned} \tag{12}$$

$$= \Delta x_0 W_0 \int \frac{d}{dx}\left[\frac{f_A(x)}{\psi_0(x)}\right]\psi_0^2 dx = 2\Delta x_0 W_0 \int f_A(x) x \psi_0(x) dx$$

The parallel dynamics is therefore asymptotically stable and exact. The use of reflected dynamics with cancellation also produces stable and exact behavior, but now it is the average position $(x_k^+ + x_k^-)/2$ that remains unchanged in the correlated diffusion step. That average position is decreased by a factor $e^{-\Delta\tau}$ at each drift step so that it approaches the origin independent of the starting point. Moreover, because of the cancellation we always have $x_k^+ < x_k^-$. It is straightforward to show that in this particular case the asymptotic distribution is exactly xe^{-x^2}, the first antisymmetric state of the harmonic oscillator. More generally, one can use a mixture of parallel and reflected dynamics, obtaining the correct answer even without using the knowledge of the nodal surface (the point $x = 0$). Note that the positive and negative walkers do not respect any particular node, ranging in principle, over the entire real line. In this one dimensional case, therefore, it is easy to go beyond the fixed-node using correlated dynamics.

3.2.2. *Many-dimensional case*

Is it possible to generalize the results for the one-dimensional harmonic oscillator for the same problem in many dimensions? In the paper by Kalos and Schmidt[17] two- and higher- dimensional problems are also discussed. To find an antisymmetric solution of the form

$$\psi_{01}(x,y) = ye^{-(x^2+y^2)} \tag{13}$$

it is enough to use pairs of walkers $\{r^+, r^-\}$ for which $x^+ = x^-$ and $y^+ > y^-$, and use either parallel or reflected dynamics, which both preserve these conditions. This is precisely analogous to the one-dimensional case.

The following state requires more thought

$$\psi_{11}(x,y) = xye^{-(x^2+y^2)} \tag{14}$$

We can recover an analogy with the one dimensional case noting that

$$\psi_{11}(x,y) = \frac{\partial^2}{\partial x \partial y}\psi_{00}(x,y) \tag{15}$$

A quartet of walkers $\{r_1^+, r_1^-, r_2^+, r_2^-\}$ satisfying the conditions:

$$\begin{array}{l} x_1^+ = x_1^- ; y_1^- < y_1^+ \\ x_2^+ < x_1^- ; y_2^+ = y_1^- \\ x_2^+ = x_2^- ; y_2^- > y_2^+ \\ x_1^+ > x_2^- ; y_1^- = y_2^+ \end{array} \tag{16}$$

gives stable and correct solutions for a parallel dynamics. In fact drift and diffusion transform a rectangle into a rectangle with the same orientation. The drift (following the ground state as guiding function) shrinks the rectangle to a point and diffusion displaces this rectangle. The mechanism is the same as in one dimension. The rectangle eventually shrinks to a point, and we can replace sums and differences of estimators with derivatives, following the same scheme as in one dimension. Reflected dynamics can be used as well. If $\{u_x, u_y\}$ is a Gaussian vector sampled for diffusion, one form of reflected dynamics is the following:

$$\begin{array}{l} x_1^+ = x_{d1}^+ + u_x; y_1^+ < y_{d1}^+ + u_y \\ x_1^- = x_{d1}^- + u_x; y_1^- < y_{d1}^- - u_y \\ x_2^+ = x_{d2}^+ - u_x; y_2^+ < y_{d2}^+ - u_y \\ x_2^- = x_{d2}^- - u_x; y_2^- < y_{d2}^- + u_y \end{array} \tag{17}$$

where the suffix d indicates the position after the drift. It can be shown that again, this dynamics gives a stable and correct result. A straightforward generalization of this argument might lead to the conclusion that we can solve a generic N-dimensional problem, (or, in the oscillator language, find an arbitrary excited state), but the complexity of the algorithm grows exponentially (we need roughly 2^M walkers, where M is the number of nodal lines of the state). This is not the case. For example, it is possible to find for the state ψ_{11} sets of pairs that give a stable result. For instance, we can consider pairs satisfying:

$$\begin{array}{l} x^+ = x^- > 0; y^+ = -y^- > 0 \\ x^+ = x^- < 0; y^+ = -y^- < 0 \end{array} \tag{18}$$

or

$$\begin{aligned} x^+ = -x^- > 0; y^+ = y^- > 0 \\ x^+ = -x^- < 0; y^+ = y^- < 0 \end{aligned} \tag{19}$$

which can be transformed into each other reflecting a walker in the origin. We can switch between the two kinds of pairs any time one pair crosses the lines $\pm x = \pm y$. This dynamics is also stable. Following the same scheme and the same kind of considerations, Kalos and Schmidt show that it is possible to solve problems as large as three oscillators in three dimensions (a nine dimensional problem) with the use of pairs and quartets. So in principle it seems to be possible to use a *limited* number of objects, and in principle *only pairs of walkers* to solve many-dimensional problems. The complexity required to solve the general problem might not grow exponentially with the dimensionality.

4. Importance Sampling plus Reflected Dynamics with Cancellation

Diffusion Monte Carlo (5) cycles through drift, diffusion, and branching steps. The details of the steps are determined by the "importance" or "guiding" function applied to the distribution. A key feature of the work on model systems of fermions described above has been the use of a spatially symmetric ground state as the importance function; with this there is no spatially dependent branching, so that ensembles of walkers can propagate as a unit, rather than breaking up and being reformed. A spatially symmetric importance function need not generate solutions to ground state problems: Equal numbers of oppositely signed walkers guarantee orthogonality to the ground state. The "drift" implied by the ground state of a harmonic potential preserves the shapes and orientations of ensembles of walkers; appropriate correlations in "diffusion" can also leave them invariant, creating stable dynamics for antisymmetric states and easily breaking the "plus-minus" symmetry .

It is not entirely obvious how to generalize this approach to treat many-body systems with arbitrary potentials. It is clear, of course, that one must relax the condition that the exact symmetric ground state be used, since it is not known. Furthermore, it seems desirable that the guiding function contain some antisymmetric components that distinguish between positive and negative walkers, and that serve to "polarize" their weighted distribution. Motivated by a desire to use ensembles of pairs of walkers, and following the ideas of the "mirror potentials" we introduce the following two special forms for the guiding function:

Let $\psi_S(\vec{R})$ be a trial function for the symmetric ground state of the system –that is, for the system treated as if the particles were bosons.

Let $\psi_A(\vec{R})$ be a trial function for the fermion ground state. Construct two guiding functions, $\psi_G^{\pm}(\vec{R})$, for the positive and negative walkers respectively as follows:

$$\psi_G^{\pm}(\vec{R}) = \sqrt{\psi_S^2(\vec{R}) + c^2\psi_A^2(\vec{R})} \pm c\psi_A(\vec{R}) \tag{20}$$

The functions $\psi_G^{\pm}$ have the following important properties that make them suitable for guiding the walkers: (a) they are both positive everywhere; (b) for small values of the parameter c, they are dominated by ψ_S, so that the differential branching of two walkers is small; (c) each function is a sum of a symmetric and an antisymmetric function, and the sign of the latter is opposite for positive and negative walkers, respectively; (d) if an odd permutation $\mathcal{P}$ is applied to the coordinates $\vec{R}$, then

$$\psi_G^{+}(\mathcal{P}\vec{R}) = \psi_G^{-}(\vec{R}) \tag{21}$$

so that the distributions developed by the positive and negative walkers map into each other.

With two different guiding functions for positive and negative walkers, the process of cancellation must be reanalyzed, since their future contributions to overlap integrals are not exactly opposite. Consider a single walker undergoing diffusion Monte Carlo in which it is advanced by integer multiples of some $\delta\tau$ using a guiding function $\psi_G(r)$. Then after a total imaginary time τ, an eigenfunction $\psi_k(\vec{R}_0)$ evolves according to

$$\psi_G(\vec{R}_0)\psi_k(\vec{R}_0) \rightarrow e^{(E_T-E_k)\tau}\psi_G(\vec{R})\psi_k(\vec{R}) \tag{22}$$

We now calculate the total expected future contribution, $F(\vec{R}_0)$, of a walker at $\vec{R}_0$ to an estimator $f(\vec{R})/\psi_G(\vec{R})$. (This follows the usual development of the idea of "forward walking".) Introduce the eigenfunction expansion of the function $\delta(\vec{R}-\vec{R}_0)$:

$$\begin{aligned}
\delta(\vec{R}-\vec{R}_0) &= \sum_k \psi_k(\vec{R})\psi_k(\vec{R}_0) \\
&= \frac{\psi_G(\vec{R})}{\psi_G(\vec{R}_0)}\delta(\vec{R}-\vec{R}_0) \\
&= \sum_k \psi_G(\vec{R})\psi_k(\vec{R})\psi_k(\vec{R}_0)/\psi_G(\vec{R}_0) \\
&\rightarrow \sum_k e^{(E_T-E_k)\tau}\psi_G(R)\psi_k(\vec{R})\psi_k(\vec{R}_0)/\psi_G(\vec{R}_0)
\end{aligned} \tag{23}$$

Then $F(\vec{R}_0)$ is obtained from Eq. 23 by multiplying by $f(\vec{R})/\psi_G(\vec{R})$ and integrating over all $\vec{R}$ and over τ from 0 to ∞.

$$F(\vec{R}_0) = \int_0^\infty \int \sum_k e^{(E_T - E_k)\tau} f(\vec{R})\psi_k(\vec{R})\psi_k(\vec{R}_0)/\psi_G(\vec{R}_0) d\vec{R} d\tau \tag{24}$$

Setting

$$f_k = \int f(\vec{R})\psi_k(\vec{R}) d\vec{R}, \tag{25}$$

we obtain

$$F(\vec{R}_0) = \frac{1}{\psi_G(\vec{R}_0)} \sum_k \frac{f_k \psi_k(\vec{R}_0)}{E_k - E_T}. \tag{26}$$

For the τ integration, we assume that E_T is slightly smaller than the smallest E_k for which f_k not equal to zero. If f_k is an antisymmetric function, then $E_T < E_F$, where E_F is the fermion energy. Finally, we have

$$F(\vec{R}_0) = \frac{F_1(\vec{R}_0)}{\psi_G(\vec{R}_0)} \tag{27}$$

where

$$F_1(\vec{R}_0) = \sum_k \frac{f_k \psi_k(\vec{R}_0)}{E_k - E_T} \tag{28}$$

is a function of $\vec{R}_0$ only.

The diffusion steps for the pairs of walkers in our algorithm are treated in a special way: First, they are correlated as follows: A vector of Gaussian random variables $\vec{U}^+$ each of mean zero and variance $\delta\tau$ is sampled as an increment for $\vec{R}^+$. $\vec{U}^+$ is reflected in the perpendicular bisector of the vector $\vec{R}^+ - \vec{R}^-$ to obtain $\vec{U}^-$, an increment for $\vec{R}^-$. In particular, $|U^+| = |U^-|$. Let

$$\begin{aligned} \vec{R}_n^+ &= \vec{R}^+ + \vec{U}^+ \\ \vec{R}_n^- &= \vec{R}^- + \vec{U}^- \end{aligned} \tag{29}$$

The second change is that the overlapping distributions of possible positions, $\vec{R}$, after diffusion are added (taking their signs into account) so as to allow some cancellation between positive and negative walkers.

Denote by

$$G(\vec{R}' - \vec{R}) = \frac{\exp[-(\vec{R}' - \vec{R})^2/(2\delta\tau)]}{(2\pi\delta\tau)^{3N/2}} \tag{30}$$

the kernel that moves a walker from $\vec{R}$ to $\vec{R}'$ in an N-body system.

Let

$$
\begin{array}{c} B^{+}(\vec{R}|\vec{R}^{+}) \\ B^{-}(\vec{R}|\vec{R}^{-}) \end{array} \tag{31}
$$

denote the branching factors that are applied to a positive and a negative walker respectively on arriving at $\vec{R}$.

We are now in a position to calculate the degree of cancellation of a pair of walkers that might arrive from $\vec{R}^{+}$ and from $\vec{R}^{-}$ at a common point $\vec{R}$, using the average future contributions from Eq. (27), Eq. (30) for the chance of arriving at $\vec{R}$, and Eq. (31) for the multiplicities found there. The expected net contribution to future scores for this pair is

$$
\begin{aligned} &\rho_f(\vec{R};\vec{R}^{+},\vec{R}^{-}) = \\ &= F_1(\vec{R}) \left\{ \frac{B^{+}(\vec{R}|\vec{R}^{+})G(\vec{R}-\vec{R}^{+})}{\psi_G^{+}(\vec{R})} - \frac{B^{-}(\vec{R}|\vec{R}^{-})G(\vec{R}-\vec{R}^{-})}{\psi_G^{-}(\vec{R})} \right\} \end{aligned} \tag{32}
$$

The condition $\rho_f(\vec{R}) > 0$ defines the region where future positive walkers are created; where $\rho_f(\vec{R}) < 0$, future walkers are negative. Thus, a positive walker at $\vec{R}_n^{+}$ will survive and be used as a positive walker in the next time step with probability

$$
\begin{aligned} &P^{+}(\vec{R}_n^{+};\vec{R}^{+},\vec{R}^{-}) = \\ &= \max\left[0, \frac{F_1(\vec{R}_n^{+})\left\{ \frac{B^{+}(\vec{R}_n^{+}|\vec{R}^{+})G(\vec{R}_n^{+}-\vec{R}^{+})}{\psi_G^{+}(\vec{R}_n^{+})} - \frac{B^{-}(\vec{R}_n^{+}|\vec{R}^{-})G(\vec{R}_n^{+}-\vec{R}^{-})}{\psi_G^{-}(\vec{R}_n^{+})} \right\}}{F_1(\vec{R}_n^{+})\frac{B^{+}(\vec{R}_n^{+}|\vec{R}^{+})G(\vec{R}_n^{+}-\vec{R}^{+})}{\psi_G^{+}(\vec{R}_n^{+})}}\right] \\ &= \max\left[0, 1 - \frac{B^{-}(\vec{R}_n^{+}|\vec{R}^{-})G(\vec{R}_n^{+}-\vec{R}^{-})\psi_G^{+}(\vec{R}_n^{+})}{B^{+}(\vec{R}_n^{+}|\vec{R}^{+})G(\vec{R}_n^{+}-\vec{R}^{+})\psi_G^{-}(\vec{R}_n^{+})}\right] \end{aligned} \tag{33}
$$

Similarly, a negative walkers survives at $\vec{R}_n^{-}$ with probability

$$
P^{-}(\vec{R}_n^{-};\vec{R}^{+},\vec{R}^{-}) = \max\left[0, 1 - \frac{B^{+}(\vec{R}_n^{-}|\vec{R}^{+})G(\vec{R}_n^{-}-\vec{R}^{+})\psi_G^{-}(\vec{R}_n^{-})}{B^{-}(\vec{R}_n^{-}|\vec{R}^{-})G(\vec{R}_n^{-}-\vec{R}^{-})\psi_G^{+}(\vec{R}_n^{-})}\right] \tag{34}
$$

Negative walkers survive only where $\rho_f(\vec{R};\vec{R}^{+},\vec{R}^{-})$ of Eq. 32 is negative, but the probability of survival is the ratio of (the negative) ρ_f to the negative density $-F_1(\vec{R})B^{-}(\vec{R}|\vec{R}^{-})G(\vec{R}-\vec{R}^{-})/\psi_G^{-}(\vec{R})$ that the walker from $\vec{R}^{-}$ brings to $\vec{R}$.

In standard diffusion Monte Carlo, the branching factors, $B^+(\vec{R}|\vec{R}^+)$ and $B^-(\vec{R}|\vec{R}^-)$ depend only on the arrival point, $\vec{R}$, and are respectively

$$B^{\pm}(\vec{R}) = \exp\left\{\delta\tau\left[E_T - \frac{H\psi_G^{\pm}(\vec{R})}{\psi_G^{\pm}(\vec{R})}\right]\right\} \tag{35}$$

In a simpler kind of diffusion Monte Carlo, which we will also use for the free particle problem, there is no drift, and the branching factors are:

$$\begin{aligned} B^+(\vec{R}|\vec{R}^+) &= \frac{\psi_G^+(\vec{R})}{\psi_G^+(\vec{R}^+)} \\ B^-(\vec{R}|\vec{R}^-) &= \frac{\psi_G^-(\vec{R})}{\psi_G^-(\vec{R}^-)} \end{aligned} \tag{36}$$

When these are used, then the survival probabilities of Eq. 33 become

$$\begin{aligned} P^+(\vec{R}_n^+;\vec{R}^+,\vec{R}^-) &= \max\left[0, 1 - \frac{\psi_G^+(\vec{R}^+)G(\vec{R}_n^+ - \vec{R}^-)}{\psi_G^-(\vec{R}^-)G(\vec{R}_n^+ - \vec{R}^+)}\right] \\ P^-(\vec{R}_n^-;\vec{R}^+,\vec{R}^-) &= \max\left[0, 1 - \frac{\psi_G^-(\vec{R}^-)G(\vec{R}_n^- - \vec{R}^+)}{\psi_G^+(\vec{R}^+)G(\vec{R}_n^- - \vec{R}^-)}\right] \end{aligned} \tag{37}$$

Appropriate branching is carried out separately for each member of the pair using these expressions for the survival probabilities. Thus, a solitary (i.e. an unpaired) walker may be spawned; on the average there are equal numbers of unpaired positive and negative walkers. A simple and effective method of turning a single walker into a pair is (with probability one half) to generate a new walker of opposite sign by interchanging the coordinates of that pair of like-spin particles that are closest to each other. This also simplifies the bookkeeping necessary to keep track of the walkers.

In these calculations we are interested in computing the eigenvalue of the Hamiltonian operator for the N-body system

$$\hat{H} = -\frac{\hbar^2}{2m}\sum_{i=1}^{N}\nabla_i + \sum_{i<j}^{N} v(r_{ij}) \tag{38}$$

corresponding to the antisymmetric ground state. Let us consider a generic antisymmetric trial function $\psi_T(\vec{R})$. An estimator for the energy for an ensemble of signed walkers is

$$E_A = \frac{\hat{H}\psi_T(\vec{R}^+) - \hat{H}\psi_T(\vec{R}^-)}{\psi_T(\vec{R}^+) - \psi_T(\vec{R}^-)} \tag{39}$$

As previously mentioned, the walker densities weighted with the functions $\psi_G^\pm$ have a stable overlap with the positive and negative part of an antisymmetric function respectively. We can therefore use configurations weighted with $\psi_G^\pm$ to compute E_A in the following way:

$$E_A = \frac{\frac{\hat{H}\psi_T(\vec{R}^+)}{\psi_G^+(\vec{R}^+)} - \frac{\hat{H}\psi_T(\vec{R}^-)}{\psi_G^-(\vec{R}^-)}}{\frac{\psi_T(\vec{R}^+)}{\psi_G^+(\vec{R}^+)} - \frac{\psi_T(\vec{R}^-)}{\psi_G^-(\vec{R}^-)}} \tag{40}$$

The denominator $\mathcal{D}$ in Eq. (40) is a quantity that can be monitored in order to check the stability of the overlap. In fact, if the populations of positive and negative walkers are distributed symmetrically in the space, then the two terms $\psi_T(\vec{R}^+)/\psi_G^+(\vec{R}^+)$ and $\psi_T(\vec{R}^-)/\psi_G^-(\vec{R}^-)$ have equal and opposite average values, so $\mathcal{D}$ averages to zero. The imaginary time to decay appreciably is of order $\tau_c = 1/(E_A - E_S)$ where E_A is the energy of the first antisymmetric state and E_S is the energy of the symmetric ground state. On the other hand, if there is a stable separation in the distribution of walkers, $\mathcal{D}$ is on average different from zero; its cumulative value grows with imaginary time. This is an important stability criterion, which guarantees that the signal to noise ratio remains constant on the average throughout the random walk. In the numerical experiments we performed, the growth rate of the denominator depended strongly on the parameter c. A value such that $c << \max[\psi_A(\vec{R})/\psi_S(\vec{R})]^{-1}$ tends to give a denominator difficult to distinguish from zero. When $c \sim \max[\psi_A(\vec{R})/\psi_S(\vec{R})]^{-1}$ the stability is more evident. This is consistent with the fact that reflected dynamics with cancellation reduces the contributions coming from the symmetric part of ψ_G (which average to zero with some variance) and only contributions from the antisymmetric part, which is proportional to c, survive.

To check our method we have chosen three different systems, each with special characteristics. A first set of calculations was performed on free fermions. The advantage of this system is that the exact results are known analytically, so a careful analysis of the convergence and of the bias of the results is possible. Another advantage is that it is straightforward to develop an algorithm without time step error. In this case it is enough to change the branching factors to:

$$B^\pm(\vec{R}_n^\pm|\vec{R}^\pm) = \psi_G^\pm(\vec{R}_n^\pm)/\psi_G^\pm(\vec{R}_{n-1}^\pm). \tag{41}$$

and to perform purely diffusive moves (without drift). For this system we assume $\hbar = m = 1$, and a density $\rho = 0.5$ As is well known, the ground state for a system of N free fermions is a determinant of plane waves, while the symmetric ground state is an arbitrary constant. The guiding function

N	E_{var}	E_{FN}	E_{ex}	E_{FDMC}
7	3.093(8)	2.912(6)	2.912712	2.900(4)
27	2.943(8)	2.834(5)	2.763316	3.13(2)

TABLE 1. Results for 7 and 27 free fermions at density 0.5. E_{var} is the variational energy, E_{FN} is the Fixed-node result, E_{ex} is the exact analytic result, and E_{FDMC} is the energy obtained with the method described in the text.

we have used for this problem is of the form

$$\psi_G^{\pm}(\vec{R}) = \sqrt{1 + c^2\varphi_A^2(\vec{R})} \pm c\varphi_A(\vec{R}) \tag{42}$$

where φ_A is a Slater determinant of one body functions $\chi_{\vec{r}_i}^{\vec{k}}$ of the following form:

$$\chi_{\vec{r}_i}^{\vec{k}} = \exp\left[i\vec{k} \cdot \left(\vec{r}_i + \lambda_B \sum_{j \neq i} \eta(r_{ij})\vec{r}_{ij} \right) \right] \tag{43}$$

and the function $\eta(r)$ has the form:

$$\eta(r) = \left(\frac{r - R_B}{R_B} \right)^3 \exp\left[- \left(\frac{r - r_B}{w_B} \right)^2 \right] \tag{44}$$

This antisymmetric wave function has a nodal structure that is different from the exact one. The value of the parameters, and in particular of λ_B, determine the deviation from a determinant of plane waves. In table I we report the results obtained from variational calculations and DMC-fixed-node for two periodic systems of 7 and 27 particles respectively, together with the exact analytic result. The parameters used in both cases are $\lambda_B = -1$,$r_B = .8907$, and $w_B = 0.5926$, while R_B is set to half the side of the simulation box. In each case we have performed several preliminary runs in order to determine a value of c for which the stability is satisfactory. In Fig. 2, upper panel, we show the cumulative value of the denominator $\mathcal{D}$ for a 7-body calculation. As it can be seen the growth is constant. The natural decay time for this particular system is $\tau = 0.049$. The time step in this simulation is $\Delta\tau = 0.004$, meaning that the denominator should start to decay after 10 time steps. There are no signs of instability for a run of order 10^6 times longer. In Fig. 2, lower panel, we plot the cumulative eigenvalue for the same problem. It can be seen that after a transient period, the eigenvalue shows a well defined convergence. The computed average differs from the exact analytic value by about three standard deviations.

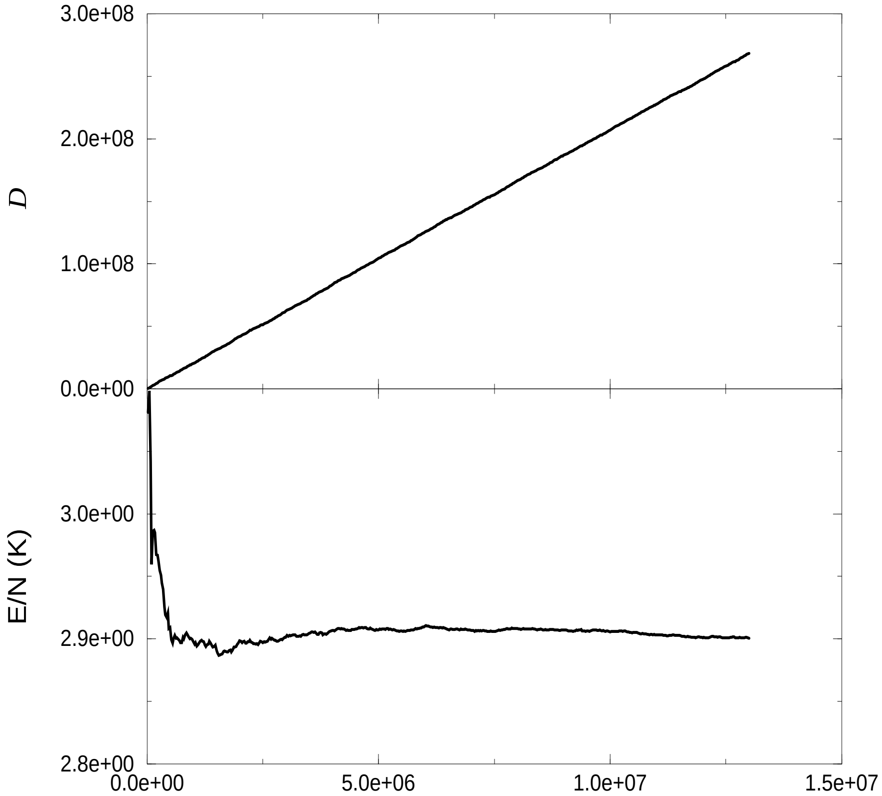

Figure 2. Cumulative value of the denominator $\mathcal{D}$ (upper panel) and cumulative value of the energy per particle in a system of 7 free fermions with periodic boundary conditions at density $\rho = 0.5$. The abscissa is the number of time steps.

This bias might arise from our use of a fixed population of walkers, in this case with only 50 pairs. In any case the results are definitely closer to the correct answer than the corresponding fixed-node result, indicating that the nodal structure has improved. For the 27-particle system we have again performed a series of runs with the same criteria. In Fig 3, upper panel, we show the denominator for one of these runs, and in Fig. 3, lower panel, the cumulative eigenvalue. The stability of the calculation is also in this case very evident, although more pronounced fluctuations appear. In particular it can be noted how the denominator undergoes abrupt changes (in both directions), which reflect on the cumulative eigenvalue. We can connect these jumps to deficiencies in the sampling having strongly branching

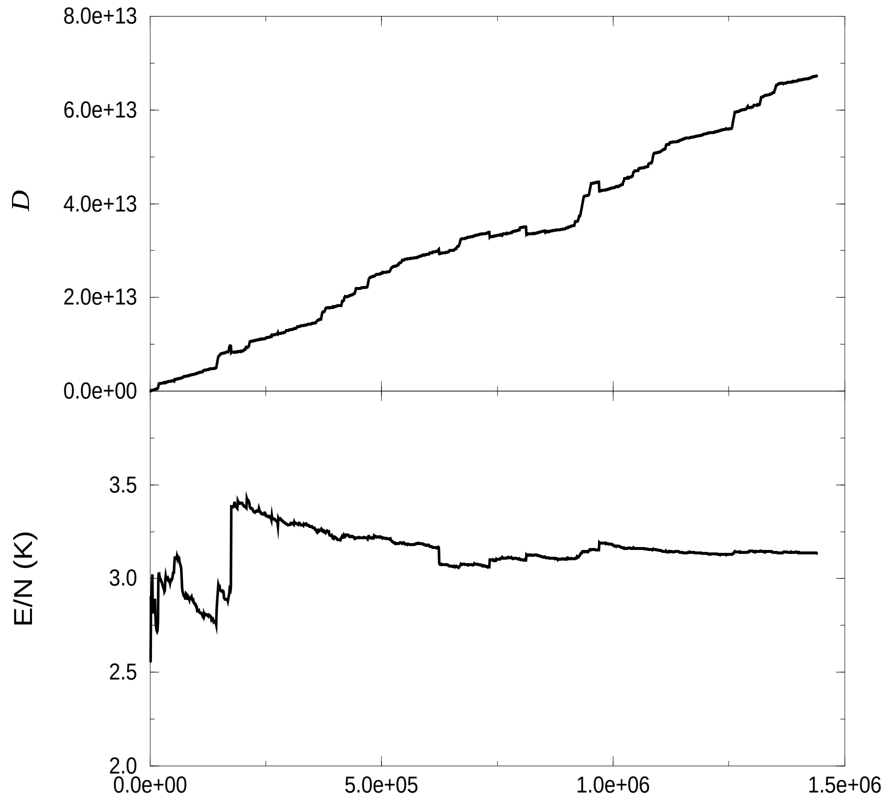

Figure 3. Cumulative value of the denominator $\mathcal{D}$ (upper panel) and cumulative value of the energy per particle in a system of 27 free fermions with periodic boundary conditions at density $\rho = 0.5$. The abscissa is the number of time steps.

configurations that temporarily dominate the population. More efficient sampling (for instance restoring drift in some form) or calculations with a larger population should contribute to remove the bias. The eigenvalue in this case has a much larger variance, and its value is clearly quite biased towards a higher value. Again, a larger population is likely to improve the agreement. In any case the important result is that the complexity of the algorithm is clearly not factorial. If it were, then a 27-body calculation would be 2.16×10^{24} longer than one for seven.

We also performed calculations for interacting systems. In particular we applied this algorithm to a system of 14 ^{3}He atoms in a box at equilibrium density. For this case the wave function must include a symmetric

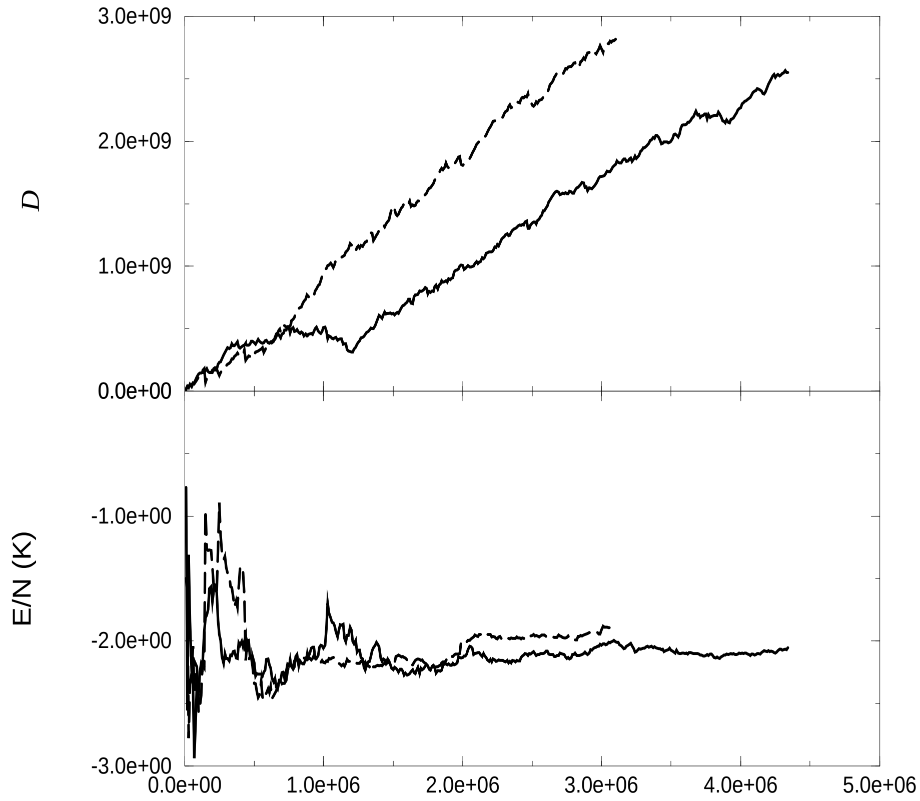

Figure 4. Cumulative value of the denominator $\mathcal{D}$ (upper panel) and cumulative value of the energy per particle in a system of 14 ^{3}He atoms with periodic boundary conditions at equilibrium density. The abscissa is the number of time steps. Solid lines refer to the run defined run A in the text and dashed lines refer to run B.

factor accounting for the pair correlations due to the repulsive part of the potential:

$$\psi_G^{\pm}(\vec{R}) = \varphi_S(\vec{R}) \left[\sqrt{1 + c^2 \varphi_A^2(\vec{R})} \pm c\varphi_A(\vec{R}) \right] \tag{45}$$

The antisymmetric part φ_A is the same as described for the free fermions case, while φ_S is a Jastrow product of the form $\varphi_S(\vec{R}) = \prod_{i<j} \exp[-(b/r_{ij})^5]$. In this case the units of length are Å, while the energies are expressed in Kelvins. The density at which we performed our calculations is $\rho = 0.0216\text{Å}^{-3}$. In this case a comparison with an exact result is impossible. We have as a reference only the fixed-node result. Also in this case we use a

relatively small number of walkers (50), and this calculation is also subject to the truncation error of a finite $\delta\tau$. We performed two main calculations for this system, which differ in the value of the parameter c in the guiding function. We label as run A the one with $c = 0.002$ and as run B the one with $c = 0.004$. In Fig. 4a we plot $\mathcal{D}$ for run A and run B; as can be seen, we have again a very stable result in both cases. However, the run A shows much more fluctuations and the growth rate is about one half than in run B. In fig 4b we show the cumulative eigenvalues for the two runs. Again, run A shows larger fluctuations in the average, while run B seems to have a smaller uncertainty. The two runs, however, converge to the values of -2.05 ± 0.06K for run A, and -1.90 ± 0.25K for run B. This two values are consistent within error bars, and both are biased towards a high value. In fact the fixed-node result for this system at the same density is $-2.33 \pm 0.01K$. Neither extrapolation in imaginary time nor a check of the dependence on the number of walkers has been done yet. We conclude that the presence of a real interatomic potential and of realistic many-body correlations do not destroy the stability of the calculations.

5. Conclusions

We have reviewed the long history of Monte Carlo approaches to exact solutions of the the Schrödinger equation for many-fermion systems. We relate the difficulty to the global nature of the antisymmetry condition, which translates into the need to break the "plus-minus symmetry", an algorithmic property that treats positive and negative walkers on an absolutely equivalent basis. We have discussed earlier methods of using correlated walkers to treat a particle in a two-dimensional box and many-dimensional harmonic oscillators, in which the use of purely geometric correlations among walkers breaks the symmetry and gives stable statistics.

We have also proposed a new method in which different guiding functions for the plus and minus walkers and a geometric correlation of the walks act together so as to be stable to very long imaginary times. The correlation used has the property of bringing together walkers in high dimensional spaces, a most desirable criterion in preventing unbounded growth of the symmetric part of the walker distribution. The method has been shown to be stable on systems of up to 27 fully polarized free fermions, on a system of 14 atoms of ^{3}He with realistic potentials, and on two atomic systems with up to four electrons. The results are somewhat biased, probably because our experimental programs depart from the exact sampling required. A fuller understanding of the sources of bias is certainly needed, but we believe that a decisive advance has been made in the solution of the "fermion Monte Carlo sign problem".

Acknowledgments

We thank Geoffrey Chester, Kevin Schmidt, David Ceperley, and Shiwei Zhang for helpful conversations. We are especially grateful to Cyrus Umrigar for his help in developing trial functions for symmetric and fermionic beryllium. The opportunity to participate in the NATO workshop in whose proceedings this paper appears served to accelerate substantially the pace of our research. One of the authors (FP) has been supported, in part, by the National Science Foundation under grant ASC 9626329. Part of this work was conducted using resources of the Cornell Theory Center (CTC), a high-performance computing center at Cornell University. CTC receives funding from the National Science Foundation, the National Center for Research Resources at the National Institutes of Health, New York State, Cornell University, and members of CTC's Corporate Partnership Program.

References

1. D.M. Ceperley and M.H. Kalos, "Quantum Many-body Problems" in *Monte Carlo Methods in Statistical Physics*, ed. by K. Binder, Springer-Verlag (1979).
2. K.E. Schmidt and M.H. Kalos, "Few- and Many-fermions Problems" in *Monte Carlo Methods in Statistical Physics*, vol. 2, ed. by K. Binder, Springer-Verlag (1984).
3. K.E. Schmidt and D.M. Ceperley, "Monte Carlo Techniques for Quantum Fluids, Solids and Droplets", in *The Monte Carlo Method in Condensed Matter Physics*, ed. by K. Binder, Topics in App. Phys., vol. 71, Springer-Verlag (1992).
4. M.H. Kalos, D. Levesque and L. Verlet, "Helium at Zero Temperature with Hard Sphere and Other Forces", Phys. Rev. **A9**, 2178 (1974).
5. J.B. Anderson, C.A. Traynor, and B.M. Boghosian, J. Chem. Phys. **95**, 7418 (1991).
6. P.J. Reynolds, D.M. Ceperley, B.J. Alder, and W.A. Lester Jr., J. Chem. Phys., **77**, 5593 (1982).
7. C.J. Umrigar, K.G. Wilson and J.W. Wilkins in *Computer Simulations Studies in Condensed Matter Physics: Recent Developments*, ed. by D.P. Landau and H.B. Schüttler, (Springer, Berlin, 1988); C.J. Umrigar, M.P. Nightingale, and K.J. Runge, J. Chem. Phys. **99**, 2865 (1993).
8. S. Moroni, S. Fantoni and G. Senatore, Phys. Rev. **B52**, 13547 (1995).
9. F. Pederiva, S.A. Vitiello, K. Gernoth, S. Fantoni and L. Reatto, Phys. Rev. B53, 15129 (1996).
10. J.Carlson and R. Schiavilla, Rev. Mod. Phys. **70**, 643 (1998).
11. M.A. Lee, K.E. Schmidt, M.H. Kalos, and G.V. Chester, Phys. Rev. Lett. **47**, 807 (1981).
12. J.B. Anderson, J. Chem. Phys. **63**, 1499 (1975).
13. J.W. Moskowitz, K.E. Schmidt, M.A. Lee, and M.H. Kalos, J. Chem. Phys. **77**, 343 (1982).
14. D.M. Ceperley and B.J. Alder, Phys. Rev. Lett. **45**, 566 (1980).
15. J. Carlson and M.H. Kalos, Phys. rev. **C32**, 1735 (1985)
16. D.M. Arnow, M.H. Kalos, M.A. Lee, K.E. Schmidt, J. Chem. Phys. **77**, 5562 (1982).
17. M.H. Kalos and K.E. Schmidt, J. Stat. Phys. **89**, 425 (1997).
18. Zhiping Liu, Shiwei Zhang and M.H. Kalos, Phys. Rev. **E50**, 3220 (1994).
19. M.H. Kalos, Phys. Rev. **E53**, 5420 (1996).